Spray electrolyte plasma polishing of GH3536 superalloy manufactured by selective laser melting

Yuliang Wu (wyl19966466736@163.com)
Xi'an Jiaotong University
Lei Wang
Jiyuan Zhao
Chao Zhang

Research Article

Keywords: Spray electrolyte plasma polishing (SEPP), Superalloy , Selective laser melting (SLM),Surface roughness · Key parameters

Posted Date: May 25th, 2022

DOI: https://doi.org/10.21203/rs.3.rs-1548334/v1

Spray electrolyte plasma polishing of GH3536 superalloy manufactured by selective laser melting

Yuliang Wu[1] · Lei Wang[1] · Jiyuan Zhao[1] · Chao Zhang[2]

Abstract

The paper deals with the studies on spray electrolyte plasma polishing (SEPP) of the GH3536 superalloy produced by selective laser melting (SLM). The theoretical operation of SEPP is shown. The GH3536 superalloy plate manufactured by SLM is used as the experimental specimen. The regularity of surface roughness on cathode feed velocity is presented. Key parameters, like distance between anode and cathode, voltage, temperature and flow rate of the electrolyte are investigated. The surface roughness, micro morphology and chemical composition of the specimen before and after polishing are detected. SEPP technology is found to decrease the surface roughness from Ra = 13.93 μm to 0.107 μm, and the specimen is smooth and bright without obvious processing traces. The oxides and other impurities on the surface of the specimen are removed, and the contents of Ni, Cr and Fe increase. The SEPP technology proposed in this paper, as a new green and efficient surface finishing technology, has the potential for further development.

Keywords Spray electrolyte plasma polishing (SEPP) · Superalloy · Selective laser melting (SLM) · Surface roughness · Key parameters

1 Introduction

Additive manufacturing has shown broad prospects in the aerospace field, such as the manufacturing of difficult-to-machine materials, Integrated manufacturing of complex structure and function and lightweight structure manufacturing [1, 2]。However, defects such as staircase effect, balling effect and powder adhesion in the additive manufacturing process will cause high roughness of formed surfaces. Therefore, additive parts generally need surface finishing to obtain high-quality surfaces to meet high-service requirements.

Superalloy shows excellent high-temperature mechanical properties, oxidation resistance and corrosion resistance. Additive manufactured superalloy parts are generally used in the key hot components of aero and rocket engine [3, 4]. At present, the main polishing methods for superalloy include mechanical grinding [5], abrasive flow polishing [6, 7], electrochemical polishing [8], etc. In the treatment of complex superalloy parts, the above polishing method can improve the surface quality significantly, however, there are inevitable problems such as surface damage, excessive surface residual stress or environmental pollution [9]. Therefore, it is urgent to develop new surface polishing technology that can be applied to complex superalloy parts.

Electrolyte Plasma Polishing (EPP) is an innovative technology used to obtain metal surfaces with low roughness and a high gloss. The mechanism of EPP is to form a vapor gaseous envelope (VGE)

✉ Lei Wang

wlei292@xjtu.edu.cn

[1] College of Mechanical Engineering, Xi'an Jiaotong Univertsity, Xi'an 710049, China
[2] National Institute Corporation of Additive Manufacturing, Xi'an , China

around the surface of the workpiece. When the voltage between the anode workpiece and the cathode is high enough, the VGE get breakdown and ionized to produce plasma discharge which function on the surface of the anode workpiece [10, 11]. The materials of micro-peaks on the metal surface are removed by a series of physical and chemical actions, which improves the surface quality of the workpiece. The advantages of EPP technology, which include high-quality surfaces, high efficiency, processing workpieces with complex shapes, no additional residual stress and low pollution, have recently attracted much attention. Some studies have also shown that after EPP treatment the surface properties such as wear resistance and corrosion resistance of workpiece are improved [12, 13]. EPP technology shows a good application prospect, which provides an opportunity to solve the finishing problem of complex additive manufactured superalloy parts.

At present, just a few research results have been published in the field of electrolyte plasma polishing, and most of them focus on the research of polishing mechanism and polishable material range [14-16]. The existing investigation results also suggest that EPP technology has a great application value in the medical field [17-19]. In 2021, Stepputat et al. [13, 20] studied the polishing effect of EPP technology on additive manufactured parts. The application of EPP technology on the inner surface of metal pipes was studied by Radkevich et al [21, 22]. However, limited by the size of the electrolyte bath and the power supply, the workpieces used in the above research are generally small-sized workpieces, there is a lack of research on workpieces with large-size and complex shape. In this paper, a Spray Electrolyte Plasma Polishing (SEPP) method for large-size and complex surfaces is proposed. The GH3536 superalloy plate produced by Selective Laser Melting (SLM) is used as the specimen for experiments. The regularity of surface roughness upon cathode feed velocity is presented. Several parameters, like distance between anode and cathode, voltage, temperature and flow rate are investigated basing on the experiments and analyses. To study the effect of SEPP technology, the surface roughness, micro morphology and chemical composition of the specimen before and after polishing are detected.

2 Methods and Materials

2.1 Theoretical mechanism

The schematic diagram of SEPP process is shown in Fig. 1. Firstly, connect the workpiece and spray head to the positive pole and negative pole of DC power supply respectively, and keep the outlet of cathode parallel to the surface to be processed of anode to provide uniform electric field. Secondly, heat the electrolyte a suitable temperature, and control the pump to spray the electrolyte to the workpiece with a certain flow. When the voltage is high enough (between 200 and 400 V). When the electrolyte contacts the anode workpiece, an instantaneous short circuit occurs and causing the electrolyzation of solution. The temperature of the anode rises rapidly, resulting the electrolyte around it vaporize instantaneously as shown in Fig. 2, and a VGE with high resistance is formed between the workpiece surface and the electrolyte, meaning that the electric circuit gets disconnected. Due to high voltage, the electric field strength is as high as 10^6 □ 10^8 V/m, causing the breakdown of the VGE and the formation of plasma, which is characterized by gas discharge. The fluctuation of the VGE makes the electrolyte constantly contact and separate from the workpiece surface [23]. Finally, the materials of micro-peaks on the metal surface are removed and the surface roughness of the workpiece is decreased.

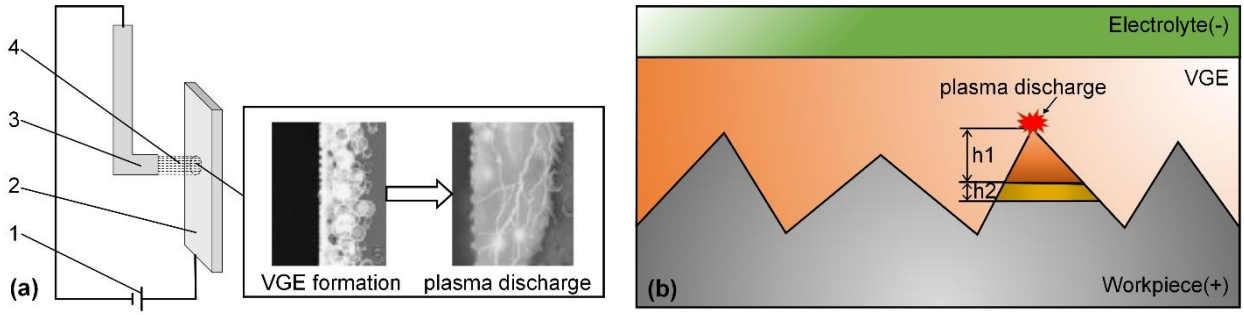

Fig.1 The schematic diagram of SEPP process: **a** the SEPP model, 1-power supply, 2-workpiece, 3-spray head, 4-electrolyte, **b** schematic diagram of workpiece surface material removal

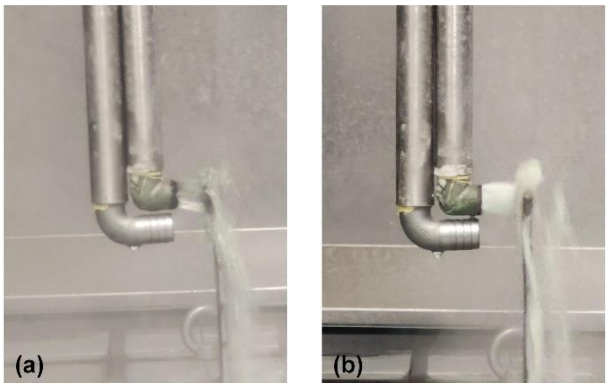

Fig.2 The vaporization of electrolyte: **a** before vaporization, **b** after vaporization

The main cause of surface material removal in the SEPP process mainly include two functions. The first is the electrochemical reaction. The active ions in the VGE electrochemically react with the metal elements on the anode surface to form oxides. Electrochemical reactions include oxygen evolution and metal oxidation. The second is the plasma discharge. Accelerated by the electric field, the electrons and ions in the VGE move to the surface of the anode. Then the kinetic energy of the particles is converted into heat energy to melt and remove the materials on the anode surface.

$$2H_2O - 4e^- \rightarrow O_2 \uparrow + 4H^+ \tag{1}$$

$$Me - ne^- \rightarrow Me^{n+} \tag{2}$$

where Me is the metal workpiece element.

The material removal rate of plasma discharge should be greater than that of the electrochemical reaction, which is the premise to achieve polishing. The higher current density at the micro-peaks on the metal surface results in a greater probability of the discharge removal effect, as show in Fig.1b, which is the key reason for the gradually leveled of metal surface. Therefore, the surface polishing of the metal is achieved.

According to the mechanism of SEPP, the polishing system can be equivalent to the circuit shown in Fig. 3, where R1 represents the resistance of the electrolyte between the cathode and anode, and R2 represents the resistance of the VGE. The resistance R is calculated according to Formula (3). R1 is a linear element conforming to Formula (4) at any current. R2 is a non-linear element. Since the VGE is almost insulated while the electrolyte is conductive, the resistance of R2 is much greater than that of R1. Therefore, the dominant voltage drops is concentrated on the VGE, which provides a high electric field strength.

$$R = \frac{\rho L}{S} \tag{3}$$

$$I = \frac{U}{R} \tag{4}$$

Where S is the cross-sectional area of instantaneous processing area on the anode surface, ρ is the resistivity of electrolyte and L is the distance between anode and cathode.

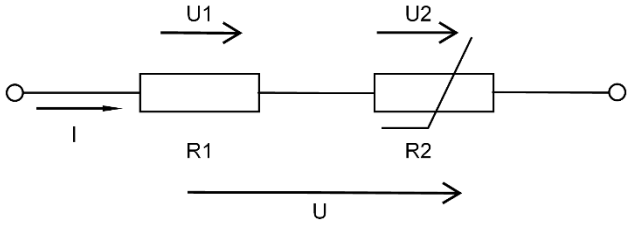

Fig.3 The equivalent circuit of SEPP system

During SEPP process, the decreasing rate of surface roughness mainly includes three aspects: the removal rate of material on the metal surface, the selective removal of materials at the micro-peaks on the surface and the pit depth caused by plasma discharge. Under certain conditions, it can be considered that the material removal rate and the pit depth are unchanged [24]. The decreasing rate of surface roughness depends on the selective removal of materials at the micro-peaks on the surface, which represent the surface roughness of the workpiece. Due to the existence of plasma discharge pit, there is a minimum surface roughness that can be obtained by SEPP technology in theory. When the surface roughness of the workpiece is equal to the theoretical minimum surface roughness, the surface roughness of the workpiece will not change with the processing time, that is, the decreasing rate of the surface roughness is equal to 0. According to the above analysis, the differential equation between the workpiece surface roughness and processing time is established:

$$\frac{dR_a}{dt} + k(R_a - R_{a\min}) = 0 \tag{5}$$

where R_a is the surface roughness at time t, $R_{a\min}$ is the theoretical minimum surface roughness.

In the SEPP process, the relationship between processing time and spray head feed velocity v is:

$$t = \frac{d}{v} \tag{6}$$

where d is the inner diameter of the spray head, d = 20mm.

Therefore, differential equation between surface roughness R_a and spray head feed velocity v:

$$\frac{dR_a}{d\frac{l}{v}} + k(R_a - R_{a\min}) = 0 \tag{7}$$

$$\lim_{v \to +\infty} R_a = R_{a0} \tag{8}$$

where R_{a0} is the initial surface roughness of the workpiece.

The general solution of equation (7) is:

$$R_a = R_{a\min} + Ce^{-\frac{kl}{v}} \tag{9}$$

According to equation (8):

$$C = R_{a0} - R_{a\min} \tag{10}$$

Let $R_{a1} = R_{a0} - R_{a\min}$, the special solution of equation (7) is:

$$R_a = R_{a\min} + R_{a1}e^{-\frac{kl}{v}} \tag{11}$$

During the SEPP process proposed in this paper, the electrolyte is sprayed on the surface of the workpiece through the spray head and the local polishing of the workpiece is realized. The cathode nozzle is connected to the end of the mechanical arm. By controlling the spray head to move along with the mechanical arm according to a certain track, the polishing of the whole area to be processed of the workpiece can be realized. For parts with different shapes and sizes, reasonably planning the moving track of spray head can theoretically achieve uniform polishing of the outer surface of the parts.

2.2 Experimental setup and material

Based on the above mechanism analysis, a set of SEPP setup was designed and built in this study, and its schematic diagram is shown in Fig. 4. The SEPP system mainly includes power supply, PLC system, electrolyte bath, mechanical arm, fixture and spray head.

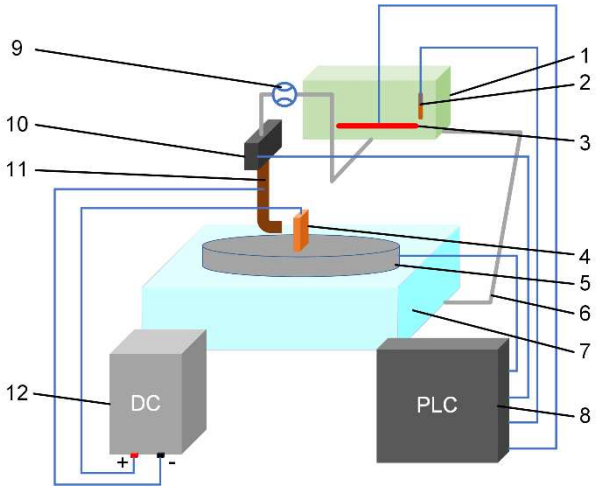

Fig.4 The SEPP setup: 1, 7-electrolyte bath, 2-temperature sensor, 3-heater, 4-workpiece, 5-fixture, 6-pipe, 8- PLC system, 9-flowmeter, 10-mechanical arm, 11-spray head, 12-power supply

SEPP technology is suitable for processing large-size parts with complex shape. To reduce the difficulty of experiment and detection, the GH3536 superalloy plates, 200 mm × 100 mm × 5 mm in size, manufactured by SLM were used as the experimental specimen. The initial surface roughness of the experimental specimen was kept as consistent as possible (around 14 μm). Prior to the experiments, the specimens were pretreated by ultrasonic cleaning to remove the surface dirt, and then dried for experiment.

For exact surface roughness of the treated specimen a roughness tester of the type MarSurf M 300C was used. Confocal laser scanning microscope (CLSM) of type Smartproof 5 was used to evaluate the three-dimensional surface morphology of the specimen. Microscopic surface morphology observation and chemical element analysis were performed through the scanning electron microscope (SEM) of the type JSM-IT500LA equipped with energy dispersive spectroscopy (EDS).

2.3 Parameters of SEPP

During the SEPP process, several parameters effect the surface quality and thus the roughness of the specimen. The electrolyte with a mass fraction of 3% and a pH of 5 was used in the experiment. In addition to the feed velocity v (i.e. polishing time per unit area to be processed) with which the cathode (the spray head) moved, the distance L (20 - 50 mm) between anode and cathode, which affects the electric field intensity, can also be varied. Furthermore, the applied voltage U (240 - 360 V), the temperature T (55-85 ℃) and the flow rate Q (5 – 17.5 L/min) can be changed.

The spray head is made of stainless steel, and its water outlet is a regular circle with an inner diameter of 20 mm. The polished specimens were ultrasonically cleaned and then dried for detection.

3 Results and Discussion

3.1 Regularity of surface roughness with cathode feed velocity

Preliminary investigation was performed to assess the influence of the velocity of the spray head to the surface roughness. The distance between anode and cathode was 30 mm, and the applied voltage was 320V. The temperature and flow rate of the electrolyte with a mass fraction of 4% was controlled at 70 ℃ and 15 L/min respectively. After SEPP process, the surface roughness of the polished specimens at different feed velocity of the spray head are shown in Table 1. Taking Formula (11) as the fitting formula, and using OriginPro software for nonlinear fitting analysis, a graphical presentation of the dependence of the surface roughness Ra upon the spray head feed velocity v is shown in Fig. 5a. The fitting results show that $R_{a\min} = 0.26999$, $R_{a1} = 15.684$, $kl = 0.89281$. It can be seen that the experimental data points are distributed near the curve and the Adjusted R-Squared is 0.99611, which means that the curve fitting effect is very good.

Table 1 Surface roughness of the specimens at different feed velocity

v （mm/s）	0.075	0.1	0.2	0.3	0.4	0.5	0.6	0.7	0.8
R_a （μm）	0.174	0.228	0.565	1.191	1.863	2.959	3.743	4.519	5.544

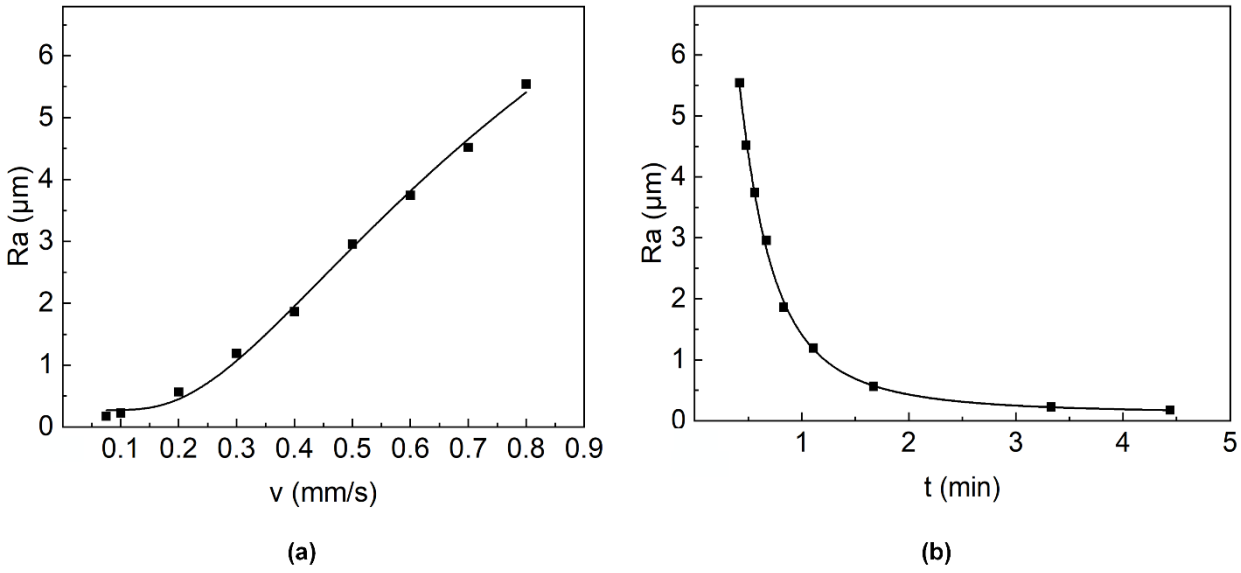

Fig.5 After SEPP process: **a** surface roughness dependence upon the spray head feed velocity, **b** surface roughness dependence upon the treatment time

The result in Fig. 5a shows that lower velocity achieves better surface roughness. This is because there is more time to remove material from the surface at a lower velocity. Different cathode feed velocities correspond to different treatment time, the dependence of surface roughness upon the treatment time is show in Fig. 5b. Due to the higher current density at the micro-peaks on the metal surface, the SEPP process starts by removing materials at the top of the surface peaks. As the metal surface is

gradually flattened, the thickness of the removed layer decreases when removing the same amount of material, i.e. h1 > h2 shown in Fig. 1b. Therefore, the surface roughness decreases rapidly at the beginning of the treatment and then continuously decreases to a constant value, which is confirmed by the results in Fig. 5.

Based on the above analysis, the regularity of the surface roughness with the cathode feed velocity was obtained. Because a smaller spray head feed velocity means a longer treatment time. In practical application, it is necessary to comprehensively consider the surface quality and polishing efficiency and select a reasonable feed velocity. For the specimens in this experiment, the optimal spray head feed velocity range is from v = 0.1 mm/s to 0.2 mm/s.

3.2 Influence of the process parameters

In this section the influences of distance L between anode and cathode, voltage U, temperature T and flow rate Q of the electrolyte on the surface roughness are presented and discussed. A series of single factor experiments were designed to study the influences of the above parameters on the surface roughness of the specimen. The experimental items and parameters are shown in Table 2.

Table 2 The experiment items and parameters

Par. / Exp.	L (mm)	U (V)	T (°C)	Q (L/min)	v (mm/s)
1	[20-50]	320	70	15	0.3
2	30	[240-360]	70	15	0.3
3	30	320	[55-85]	15	0.3
4	30	320	70	[5-17.5]	0.3

The applied distance L between anode and cathode is changed from 20 to 50 mm in 5 mm steps. Fig.6 shows the surface roughness R_a under different distance L. In the range of 25-50 mm, the variation of the surface roughness decreases with decreasing distance. It can be explained by the fact that the electric field and the current (Fig. 3) increases with the decrease of the distance between electrodes. And this is an indicator that more materials are removed with a current density between 0.2 and 0.5 A/cm^2 with increasing current and thus a lower surface roughness is achieved. When the distance between anode and cathode is decreased to 20 mm, the further enhancement of the electric field leads to the violent fluctuation of VGE. A strong spark as shown in Fig.7 was observed during the experiment. The polishing process becomes unstable, resulting a higher surface roughness compared to the result when the distance is 25 mm.

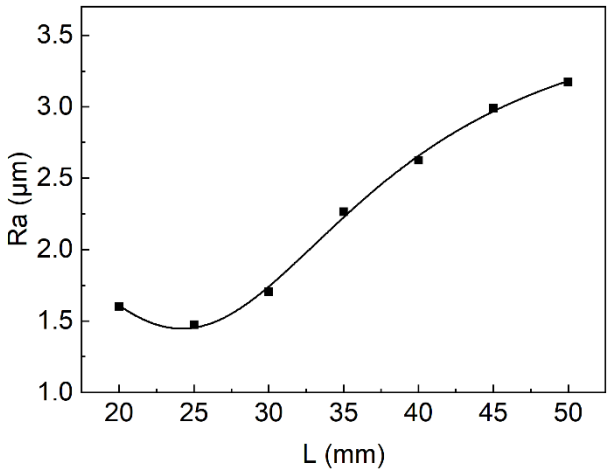

Fig.6 Surface roughness dependence upon the distance between anode and cathode

Fig.7 Strong spark observed during the experiment

As shown in Fig.8, the curve of surface roughness changing with voltage U reflects the variation characteristics of the surface roughness when increasing voltage from 240 V to 360 V. When the applied voltage is lower than 300 V, the surface roughness decreases with the increase of voltage. Once the voltage exceeds 320 V, increasing the voltage will lead to the increase of the surface roughness. The value of the applied voltage affects the energy of the particles reaching the surface of the anode, thus affecting the material removal rate of the metal surface. When the applied voltage is lower, the material removal rate increases with the increase of the voltage, and the obtained surface roughness decreases. However, rising voltage will increase the amount of heat released from the anode, causing the VGE thicker and more stable and thus decreasing the current. The lower current means less material removal rate, and the achievable surface roughness increases.

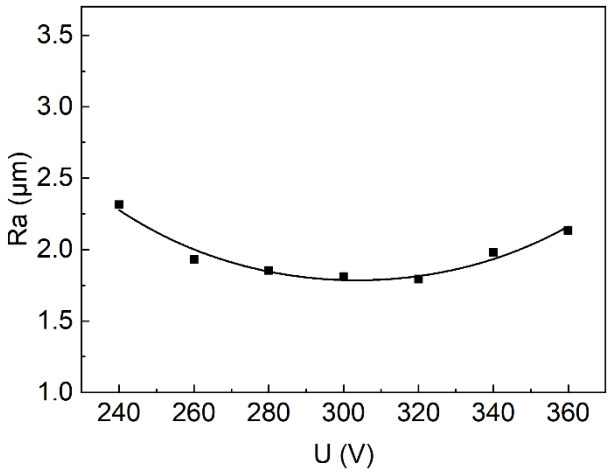

Fig.8 Surface roughness dependence upon the applied voltage

It can be seen from Fig.9 that when the temperature range is 70 – 80 ℃, the minimum surface roughness is achieved. The energy of each treated area is a certain value because of the moving of the cathode. When the temperature is lower than 70 ℃, the energy is not enough to form a continuous and stable VGE, causing the poor surface quality of the treated specimen. When the temperature increases to 85 °C, the electrolyte appears local boiling, and some electrolyte components will quickly decompose and volatilize, which weakens the polishing effect.

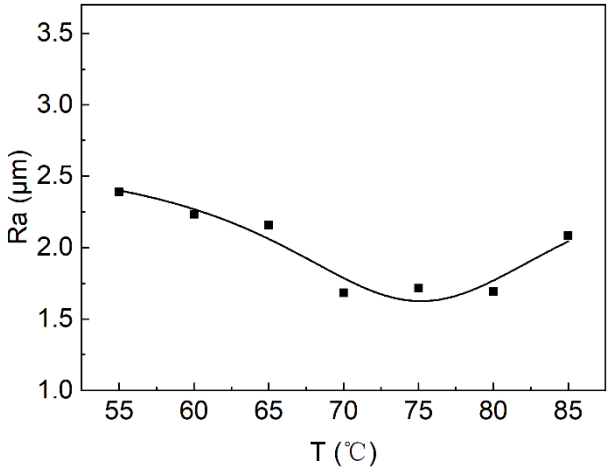

Fig.9 Surface roughness dependence upon the electrolyte temperature

Figure 10 shows that the surface roughness shows a decreasing trend when the flow rate Q of the electrolyte increases from 5 L/min to 12.5 L/min. And more area is being polished with increasing flow rate. A further increase of the flow rate destroys the lasting and stable of the VGE. The SEPP process becomes unstable, resulting in the increase of achievable surface roughness of the treated specimen.

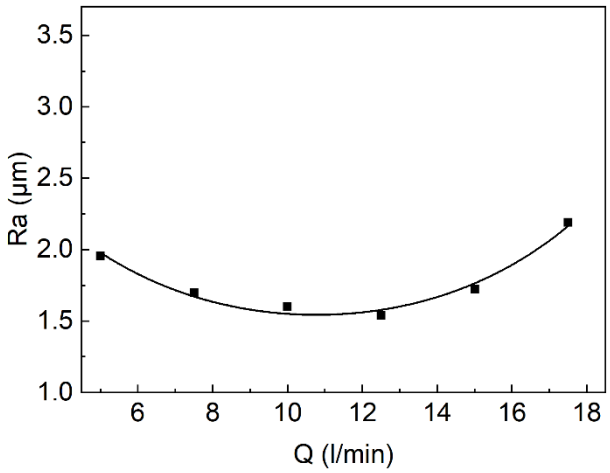

Fig.10 Surface roughness dependence upon the electrolyte flow rate

3.3 Surface properties

Based on the results of the above experiments, a new SEPP experiment was carried with the parameters shown in Table 3.

Table 3 The experiment parameters

L	*U*	*T*	*Q*	*v*
(mm)	(V)	(℃)	(L/min)	(mm/s)
0.1	25	320	75	12.5

The surface roughness Ra and Rz of pre-polishing (PP) specimen and SEPP treated specimen are shown in Table 4. It can clearly be seen that the SEPP process significantly decreases the surface roughness from Ra = 13.93 μm to 0.107 μm, while the surface roughness Rz is reduced from 78.18 μm to 1.130 μm. Fig.11 shows the micro-profiles of the PP and the SEPP surface. The CLSM images of the PP and the SEPP surface are presented in Fig.12. The results in Fig.11 and Fig.12 show that the materials of the surface micro-peaks were removed by SEPP process, and a flattened surface was achieved.

Table 4 The surface roughness of the PP and the SEPP surface

Roughness / Specimen	Ra/μm	Rz/μm
PP	13.93	78.18
SEPP	0.107	1.130

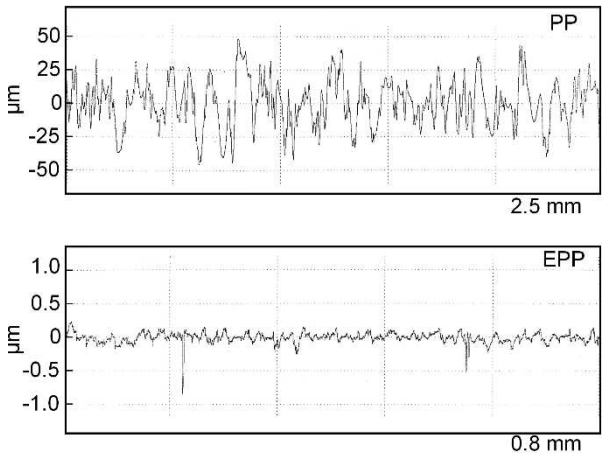

Fig.11 Comparation of the micro-profiles of the of the PP and the SEPP surface

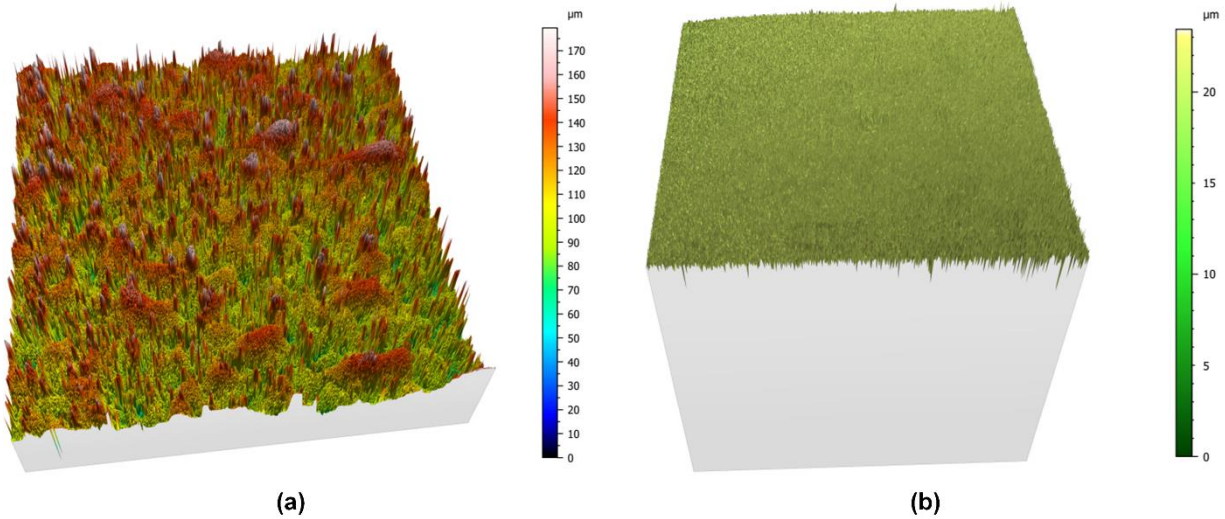

Fig.12 The CLSM images of (a) the PP surface and (b) the SEPP surface

As shown in Fig.13a, there is a large amount of spherical powder on the surface of the specimen, which is a typical defect the additive parts. Compare the SEM results in Fig. 13a and Fig. 13b, it is obvious that both the micro-peaks and the spherical powders were removed, and there were no machining traces on the treated surface. This is an indicator that the SEPP technology can significantly improve the surface quality of the specimen, resulting in a very smooth surface.

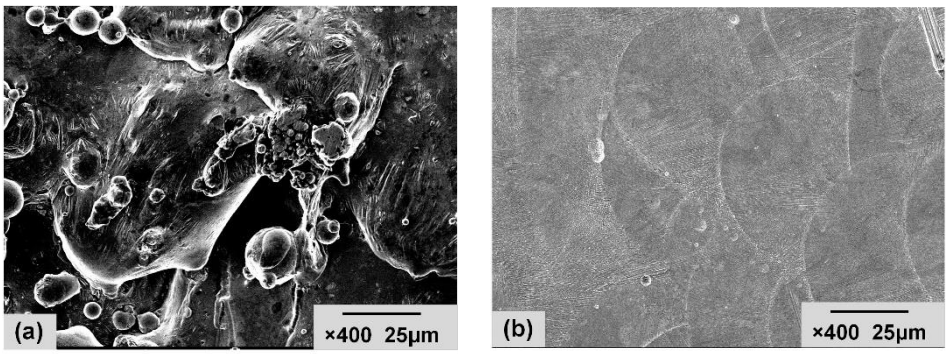

Fig.13 The SEM images (× 400) of (a) the PP surface and (b) the SEPP surface

Comparing the results in Fig. 14a and Fig. 14b, after SEPP treatment, the O on the surface of the specimen disappeared, and the content of Al decreased. It can be explained by the fact that the oxide (e.g. Al_2O_3) on the metal surface was removed. Further analysis of the EDS spectrum shows that the content of Ni, Cr, and Fe increased. This is because that after polishing, the oxides and dirt on the surface were removed, so that more Ni, Cr, Fe and other elements were exposed on the surface. The Cr and Fe are more active than Ni. During SEPP process, the active ions in the VGE will preferentially react with elements with higher activity, and then the reaction products are removed by discharge. Therefore, the detected Ni content increased more than Fe and Cr.

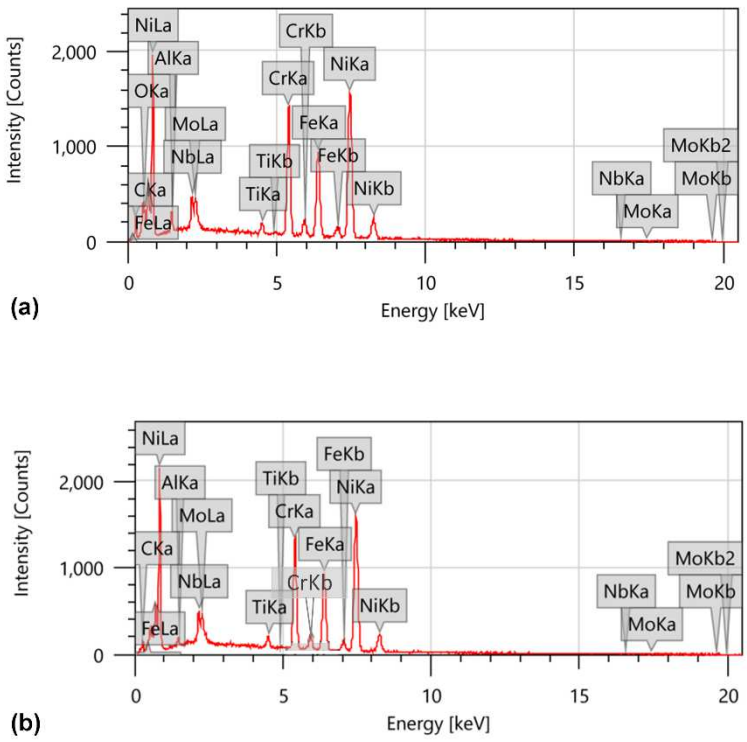

Element	Mass%	Atom%
Ni	46.84	35.94
Cr	18.14	15.72
Fe	17.28	13.94
Nb	4.40	2.13
Mo	2.93	1.37
C	5.42	20.34
Ti	1.05	0.99
Al	1.35	2.25
O	2.60	7.32

Element	Mass%	Atom%
Ni	50.75	44.61
Cr	18.53	18.39
Fe	17.93	16.57
Nb	4.97	2.76
Mo	2.99	1.61
C	3.23	13.87
Ti	1.05	1.13
Al	0.55	1.05

Fig.14. The EDS spectrums of (a) the PP surface and (b) the SEPP surface

4 Conclusions

In this paper, a method for spray electrolyte plasma polishing of large-size and complex surfaces was proposed and the experimental results were presented. The main findings of this study can be summarized as follows.

1. The regularity of surface roughness on cathode feed velocity v was analyzed. A smaller spray head feed velocity means a longer treatment time. A significant reduction of the surface roughness can be achieved when the feed velocity is 0.1 mm/s. Further slowing down the feed velocity will continually decrease the surface roughness to a constant value.
2. Key parameters, like distance between anode and cathode, voltage, temperature and flow rate of the electrolyte were investigated. The optimal parameters are L = 25 mm, U = 300 - 320 V, T = 70 - 80 °C, Q = 10 - 12.5 L/min.
3. In addition, SEPP technology was found to decrease the surface roughness from Ra = 13.93 μm to 0.107 μm, and the treated specimen is smooth and bright without obvious processing traces. the oxides and dirt on the surface were removed and the content of Ni, Cr, and Fe increased.

Author contribution Yuliang Wu, Lei Wang, Jiyuan Zhao and Chao Zhang contributed to the conception of the study; Yuliang Wu and Chao Zhang performed the experiment; Yuliang Wu contributed significantly to analyses and paper preparation; Lei Wang and Jiyuan Zhao helped perform the analysis with constructive discussions.

Funding The authors declare that no funds, grants, or other support were received during the preparation of this manuscript.

Availability of data and materials Not applicable.

Code availability Not applicable.

Declarations

Ethics approval Not applicable.

Consent to participate Not applicable.

Consent for publication Not applicable.

Conflict of interest The authors declare that they have no competing interests.

References

1. Uriondo A, Esperon-Miguez M, Perinpanayagam S (2015) The present and future of additive manufacturing in the aerospace sector: A review of important aspects. Proceedings of the Institution of Mechanical Engineers Part G-Journal of Aerospace Engineering 229(11): 2132-2147. https://doi.org/10.1177/0954410014568797
2. Lu BH (2020) Additive ManufacturingCurrent Situation and Future. China Mechanical Engineering 31(1): 19-23.
3. Zhang XS, Chen YJ, Hu JL (2018) Recent advances in the development of aerospace materials. Progress in Aerospace Sciences 97: 22-34. https://doi.org/10.1016/j.paerosci.2018.01.001
4. Darolia R (2019) Development of strong, oxidation and corrosion resistant nickel-based superalloys: critical review of challenges, progress and prospects. International Materials Reviews 64(6): 355-380. https://doi.org/10.1080/09506608.2018.1516713
5. Miao Q, Ding WF, Gu YL, Xu JH (2019) Comparative investigation on wear behavior of brown alumina and microcrystalline alumina abrasive wheels during creep feed grinding of different nickel-based superalloys. Wear 426: 1624-1634. https://doi.org/10.1016/j.wear.2019.01.080
6. Yu TB, Guo XP, Wang ZH, Xu PF, Zhao J (2019) Effects of the ultrasonic vibration field on polishing process of nickel-based alloy Inconel718. Journal of Materials Processing Technology 273: 116228. https://doi.org/10.1016/j.jmatprotec.2019.05.009
7. Han S, Salvatore F, Rech J, Bajolet J (2020) Abrasive flow machining (AFM) finishing of conformal cooling channels created by selective laser melting (SLM). Precision Engineering-Journal of the International Societies for Precision Engineering and Nanotechnology 64: 20-33. https://doi.org/10.1016/j.precisioneng.2020.03.006
8. Pyka G, Burakowski A, Kerckhofs G, Moesen M, Van Bael S, Schrooten J, Wevers M (2012) Surface Modification of Ti6Al4V Open Porous Structures Produced by Additive Manufacturing. Advanced Engineering Materials, 2012, 14(6): 363-370. https://doi.org/10.1002/adem.201100344
9. Liu D, Shi YY, Lin XJ, Xian C (2019) Study on improving surface residual stress of polished blade after polishing based on two-stage parameter method. The International Journal of Advanced Manufacturing Technology 100: 1491-1503. https://doi.org/10.1007/s00170-018-2758-3
10. Huang Y, Wang CY, Ding F, Yang Y, Zhang T, He XL, Zheng LJ, Li NT (2021) Principle, process, and application of metal plasma electrolytic polishing: a review. International Journal of Advanced

Manufacturing Technology 114(7-8): 1893-1912. https://doi.org/10.1007/s00170-021-07012-7

11. Belkin PN, Kusmanov SA, Parfenov EV (2020) Mechanism and technological opportunity of plasma electrolytic polishing of metals and alloys surfaces. Applied Surface Science Advances 1: 100016. https://doi.org/10.1016/j.apsadv.2020.100016
12. Narayanan TSNS, Kim J, Park HW (2020) High performance corrosion and wear resistant Ti-6Al-4V alloy by the hybrid treatment method. Applied Surface Science 504: 144388. https://doi.org/10.1016/j.apsusc.2019.144388
13. Seo B, Park HK, Kim HG, Kim WR, Park K (2021) Corrosion behavior of additive manufactured CoCr parts polished with plasma electrolytic polishing. Surface & Coatings Technology 406: 126640. https://doi.org/10.1016/j.surfcoat.2020.126640
14. Nestler K, Bottger-Hiller F, Adamitzki W, Glowa G, Zeidler H, Schubert A (2016) Plasma Electrolytic Polishing - an Overview of Applied Technologies and Current Challenges to Extend the Polishable Material Range. 18th Cirp Conference on Electro Physical and Chemical Machining (Isem Xviii) 42: 503-507. https://doi.org/10.1016/j.procir.2016.02.240
15. Parfenov EV, Farrakhov RG, Mukaeva VR, Gusarov AV, Nevyantseva RR, Yerokhin A (2016) Electric field effect on surface layer removal during electrolytic plasma polishing. Surface & Coatings Technology 307: 1329-1340. https://doi.org/10.1016/j.surfcoat.2016.08.066
16. Danilov I, Hackert-Oschatzchen M, Zinecker M, Meichsner G, Edelmann J, Schubert A (2019) Process Understanding of Plasma Electrolytic Polishing through Multiphysics Simulation and Inline Metrology. Micromachines 10(3): 214. https://doi.org/10.3390/mi10030214
17. Zeidler H, Boettger-Hiller F, Edelmann J, Schubert A (2016) Surface Finish Machining of Medical Parts Using Plasma Electrolytic Polishing. Second Cirp Conference on Biomanufacturing 49: 83-87. https://doi.org/10.1016/j.procir.2015.07.038
18. Smyslova MK, Tamindarov DR, Plotnikov NV, Modina IM, Semenova IP (2018) Surface electrolytic-plasma polishing of Ti-6Al-4V alloy with ultrafine-grained structure produced by severe plastic deformation. IOP Conference Series: Materials Science and Engineering 461: 012079 (6 pp.). https://doi.org/10.1088/1757-899X/461/1/012079
19. Navickaite K, Ianniciello L, Tusek J, Engelbrecht K, Bahl CRH, Penzel M, Nestler K, Bottger-Hiller F, Zeidler H (2021) Plasma Electrolytic Polishing of Nitinol: Investigation of Functional Properties. Materials, 14(21): 6450. https://doi.org/10.3390/ma14216450
20. Stepputat VN, Zeidler H, Safranchik D, Strokin E, Bottger-Hiller F (2021) Investigation of Post-Processing of Additively Manufactured Nitinol Smart Springs with Plasma-Electrolytic Polishing. Materials 14(15): 4093. https://doi.org/10.3390/ma14154093
21. Radkevich MM, Kuzmichev IS (2021) Technological schemes for elongated foramen internal surface finishing by forced electrolytic-plasma polishing. Advances in Mechanical Engineering Selected Contributions from the Conference ldquoModern Engineering: Science and Educationrdquo Lecture Notes in Mechanical Engineering (LNME): 102-11. https://doi.org/10.1007/978-3-030-62062-2_11
22. Cornelsen M, Deutsch C, Seitz H (2017) Electrolytic Plasma Polishing of Pipe Inner Surfaces. Metals 8(1): 12. https://doi.org/10.3390/met8010012
23. Zhou CQ, Su HH, Qian N, Zhang Z, Xu JH (2022) Characteristics and function of vapour gaseous envelope fluctuation in plasma electrolytic polishing. International Journal of Advanced Manufacturing Technology 119: 7815-7825. https://doi.org/10.1007/s00170-021-08606-x
24. Wang J, Suo LC, Fu YL, Guan L (2012) Study on material removal rate of electrolysis and plasma

polishing. 2012 IEEE International Conference on Information and Automation, Shenyang, China. IEEE 917–922. https://doi.org/10.1109/ICInfA.2012.6246913